Available online at www.sciencedirect.com

SciVerse ScienceDirect

Ceramics International 38 (2012) 1043–1050

CERAMICS INTERNATIONAL

www.elsevier.com/locate/ceramint

Fabrication of novel multilayer Al_2O_3–(m-ZrO_2)/t-ZrO_2 fibrous ceramics composites

Swapan Kumar Sarkar, Byong Taek Lee *

Department of Biomedical Engineering and Materials, School of Medicine, Soonchunhyang University, 366-1 Sangyoung-dong, Cheonan City, Chungnam 330-090, South Korea

Received 20 July 2011; received in revised form 11 August 2011; accepted 11 August 2011
Available online 19 August 2011

Abstract

A novel layered microstructure in the Al_2O_3/ZrO_2 composites system was fabricated by the multipass extrusion method. The microstructure consisted with very fine alternate lamina of Al_2O_3–(m-ZrO_2) and t-ZrO_2. The composites were designed in such a way that a small group of 7 cylindrical alternate layers of Al_2O_3–(m-ZrO_2) and t-ZrO_2 made a concentric microgroup around 40 μm in diameter, with a common boundary layer between the adjacent groups. The thickness of both layers was around 2–3 μm. The microstructure was unidirectionally aligned throughout the composites. The composite microstructure was fibrous due to the unidirectional orientation of these microgroups. Detailed microstructure of the fabricated composites was characterized by SEM. The effect of the concentric layered microstructure on mechanical behavior was discussed. Material properties such as density, bending strength, Vickers hardness and fracture toughness were measured and evaluated depending on different sintering temperatures.

Keywords: A. Extrusion; B. Composites; B. Microstructure; D. Al_2O_3; D. ZrO_2

1. Introduction

Al_2O_3–ZrO_2 ceramics have been used extensively as an industrial material such as wear and corrosion resistance components, high temperature application and environmental filter as well as a bio-implant material because of their excellent chemical and thermal stability, strength and biocompatibility [1,2]. In case of high temperature and structural application an important concern is the mechanical properties of ceramics. However, like other ceramics the Al_2O_3 exhibits low fracture toughness, which limits its usability. Many efforts have been made in the past to improve the fracture toughness as well as the mechanical reliability of the ceramics. Attempts were taken through the exploitation of the reinforcing action of grain anisotropy or second phases or the promotion of the crack shielding effects associated to phase-transformation or micro-cracking to attain higher fracture toughness [3]. The advancement on microstructure related mechanism for crack-shielding along with new microstructure design has made significant progress in terms of mechanical behavior of ceramics [4–6]. Layered or laminated microstructure has been considered as a relatively simple and inexpensive approach, showing interesting results and as a valid alternative to more sophisticated processes. Drastic increase in strength and fracture toughness has been achieved in Al_2O_3/ZrO_2 laminar composites because of various crack-shielding phenomena related to the presence of the layers (delamination, crack deflection, etc.) [7–9]. The laminated microstructure can induce and modify the residual stress and its distribution within the composites, which can improve the material properties [10]. The differences in the thermal expansion co-efficient and elastic modulus of the materials of the alternate lamina originate the residual stresses (tensile and compressive stresses), where these stresses are built up homogeneously in the whole volume of the layered composites instead of localized stress concentration zones. It is possible to develop high compressive and tensile residual stresses in successive thin layers [11]. Specially in Al_2O_3/ZrO_2 composites the unique property of t-ZrO_2 to undergo tetragonal to monoclinic phase transformation can attribute to a volume change due to their density difference which is too responsible

* Corresponding author. Tel.: +82 41 570 2427; fax: +82 41 577 2415.
E-mail address: lbt@sch.ac.kr (B.T. Lee).

0272-8842/$36.00
doi:10.1016/j.ceramint.2011.08.029

for the development of residual stresses [12,13]. It was reported that the presence of layers can influence the transformation zone of the layers in phase transforming ceramics like ZrO_2 [4]. High temperature creep behavior has been found to be significantly altered in case of layered microstructure compared to the conventional duplex microstructure of Al_2O_3–ZrO_2 composites, due to the presence of distinct and well developed interface [14]. This kind of microstructure has exhibited enhanced ductility and creep resistance. In the Al_2O_3 system the high temperature grain growth is a concern for the material properties degradation especially for hardness, creep behavior, fracture toughness, etc. Grain growth in high temperature environment is due to the thermal diffusion of the atoms or ions at grain boundary layer. Incorporation of a second phase can restrict this successfully by denying the adjacency of the same phase and creating a barrier. In view of this, a very fine laminated microstructure with the laminate thickness in the order 1 μm and consequently having very fine geometric isolation of the adjacent phases can successfully restrict the grain growth of monolithic phase across the laminate thickness. However, it is to be noted that grain can grow without any restriction along the direction of laminate plane which can be lessened by a conventional duplex type of microstructure. This aspect is highly beneficial if the material is required to withstand a prolonged high temperature exposure in mechanical load bearing condition. Fabrication of laminated structures employed the conventional processing routes, such as tape casting [11,15], sequential slip casting [16–18], rolling [19], electrophoretic deposition [20,21], colloidal technique [4], etc. Different types of casting methods are the most common of these. Controlling the microstructure with fine laminate is very difficult with these processes. Moreover, the lamina in the composites were mostly flat. The freedom of geometric change of the microstructure is restricted by the method. The parallel and flat lamina in these systems were directed in one direction and resulted in anisotropic characteristics in the composites. Properties like bending strength and fracture toughness values depend on the orientation and configuration of the lamina [22,23]. In case of laminated microstructure the in plane and normal to plane mechanical properties are considerably different due to the orientation of the lamina. Usually the laminated composites have coarse microstructure with laminate thickness in the order of 100 μm. This along with the fact that residual compressive and tensile stresses are developed alternately across the lamina, usually having a maximum at some planes along the lamina, make it plausible that the non uniformity of the material properties is fair enough even in the in-plane direction. From this point of view a micro-level modification with a finer microstructure can reduce the space distribution of the heterogeneous localization of property values and make them more uniform. However, it is to be noted that this anisotropy itself contributes to the fracture toughening of the composites by various mechanisms like crack arresting, crack bifurcation, etc. Considering the above factors, a multilayered cylindrical microstructure can be seen as a potential way to reduce this in-homogeneity due to the symmetry of this structure in the radial direction but still retaining the advantages of the laminated microstructure. The co-axially layered cylindrical microstructure can be seen as a new way to moderate the features of the conventional flat laminated ceramics with the new advantage of dimensional symmetry. This type of microstructure exhibits the same mechanism for the crack deflection and crack arresting by the lamina. Moreover, the curved interface of the cylindrical layers interacts with cracks, which are generally straight in ceramics system if not interrupted otherwise, and can affect on the crack propagation behavior to improve the fracture toughness.

Composites with the cylindrical concentric laminated microstructures with very fine dimension were rarely reported to date [24]. In this work, we fabricated a novel microstructure with concentric laminates of t-ZrO_2 and Al_2O_3–(m-ZrO_2) by the multi-extrusion process. The microstructure was designed with concentric lamination groups directed in a common axial direction. Each laminated group consists of 6 coaxial lamina [three of t-$ZrO_2$and three of Al_2O_3 (25% m-ZrO_2)] and a thick common boundary laminate of t-ZrO_2between two groups. A central Al_2O_3 (25% m-ZrO_2) fiber (referred to as Al_2O_3–(m-ZrO_2) from now on) acts as the axial core of the unit cell. The detailed microstructural features and material properties were evaluated for the composites system.

2. Experimental procedure

The starting powders used in this experiment were Al_2O_3 (AKP-50, average diameter 300 nm, Sumimoto, Japan), monoclinic Zirconia (m-ZrO_2) (TZ-0Y, average diameter 80 nm, Tosoh, Japan) and tetragonal Zirconia (t-ZrO_2) (TZ-3Y, average diameter 80 nm, Tosoh, Japan). Al_2O_3 powder with 25 vol% of m-ZrO_2 was mixed by ball mill for 24 h to form a homogeneous mixture. The ball-mixed Al_2O_3–(25% m-ZrO_2) powder and t-ZrO_2 powders were shear-mixed separately with a polymer binder (Ethylene Vinyl Acetate (EVA) (Elvax 250 and Elvax 210, Dupont, USA)) in a heated blender (Shina Platec. Co., Suwon, South Korea) at a temperature of 120 °C. To decrease the viscosity and enhance the fine mixing, stearic acid (Daejeon Chemical Company, Korea) was used. The polymer-laden t-ZrO_2 and Al_2O_3–mZrO_2 plastic materials were then extruded in a heated die separately to obtain green filaments 2 mm in diameter and 8 mm in length. These two kinds of filaments were then arranged in a cylindrical steel die of 30 mm in diameter. The t-ZrO_2 filaments were arranged against the die wall making the outer layer. The next layer inside was made with the Al_2O_3–(m-ZrO_2) filaments. Successive inner layers were made with alternate t-ZrO_2 and Al_2O_3–(m-ZrO_2) filaments filling the entire die. Alternate layers of t-ZrO_2 filaments and Al_2O_3 (m-ZrO_2) filaments were arranged starting from the die wall, as shown in Fig. 1. Three layers of Al_2O_3–(m-ZrO_2) filaments were arranged sandwiched within four t-ZrO_2 filament layers. A total of 7 alternate layers of t-ZrO_2 and Al_2O_3–(m-ZrO_2) filaments made up the entire arrangement. This arrangement of the alternate layers of t-ZrO_2 and Al_2O_3–(m-ZrO_2) constitutes the primary microstructure of concentric multilayer. The arrangement was warm pressed for compaction and extruded at 120 °C at a speed of 7 mm/min. The obtained

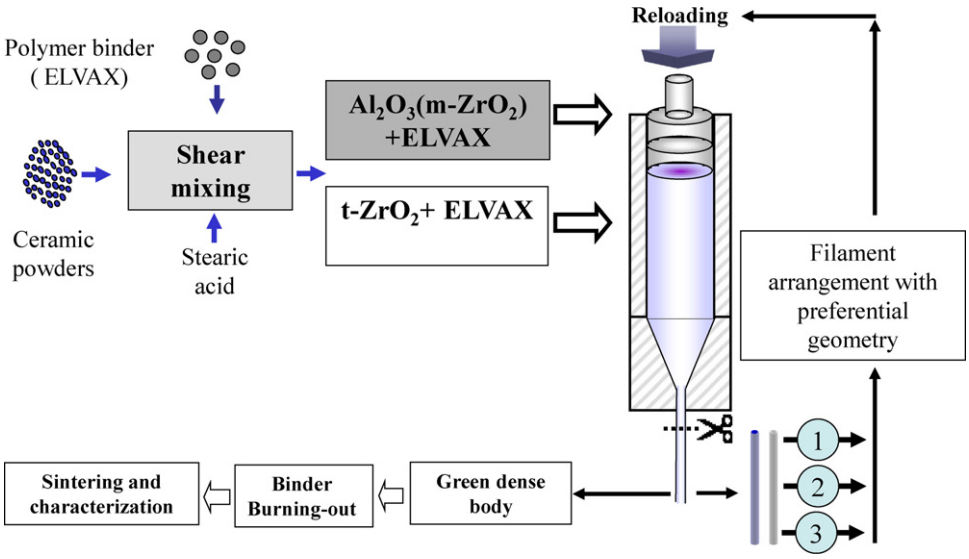

Fig. 1. Schematic diagram of multipass extrusion process.

1st passed filaments were 3.5 mm in diameter. This 1st pass filaments were reloaded in the same steel die, where there were 61 filaments, and then extruded to get the 2nd passed filaments with the same 3.5 mm diameter. The 3rd extrusion was carried out in the same way with 61 of the 2nd passed filaments loading in the same die to get the final extruded green body. The final green composite filament diameter was 3.5 mm in diameter. To remove the polymer binder from the green body it was heated very slowly up to 700 °C with a slow heating rate under a flowing nitrogen atmosphere and a subsequent burning out was carried out at 1000 °C at air atmosphere for 2 h. The samples were then sintered at 1400–1550 °C for 2 h in air. The density of the sintered Al_2O_3–(m-ZrO_2)/t-ZrO_2 bodies was measured using the Archimedes method. The Vickers hardness was measured using Vickers hardness testing machine (HV-112, Akashi, Japan) with a load of 5 kg for at least 10 readings per sample. Bending strength was measured using the four point bending strength measurement system with as received sintered cylindrical composites without any further preparation because of the smooth surface. At least 8 samples were used for each of the mechanical property measurement. The span length was 20 mm for the outer pair of span and crosshead speed was 0.1 mm/min. Due to the geometry of the sample, instead of the more accurate SENB method to determine the fracture toughness, we investigated the fracture toughness by a less reliable but easy to do method named the Vickers indentation method using the Evan's equation as follows.

$$K_{1C} = 0.16Ha^{1/2}(c/a)^{-3/2}$$

where H = Vickers hardness, a = half of indentation diagonal, c = half of crack length from indentation center.

The equation was chosen to follow the trend of variation of fracture toughness values depending on sintering temperature and direction of the microstructure orientation (along the axial and radial plan of the cylindrical unit microstructure). Although the fracture toughness values do not reflect the actual values due to the inherent margin of deviation for the equation we used, but it can be used for the direct comparison with the same composites system having different microstructure that we developed previously in our group [25,26]. The microstructure of the composites was examined using SEM (FE-SEM, JSM 6335F, JEOL, Tokyo, Japan).

3. Results and discussion

Fig. 2 shows the SEM (a) cross sectional and (b) longitudinal images of the 2nd passed multilayered Al_2O_3–(m-ZrO_2)/t-ZrO_2 sintered body. The black and the white contrasts are the Al_2O_3–(m-ZrO_2) and t-ZrO_2 lamina, respectively. Fig. 2(a) shows a unit cell of the microstructure where all the lamina encircled a central Al_2O_3–(m-ZrO_2) fiber as the axis. Alternate layers of Al_2O_3–(m-ZrO_2) and t-ZrO_2 encircled the central axis. The interface of the lamina was wavy, and the unit cell apparently took a hexagonal shape. This shape formation is attributed to the die geometry and filament arrangement in the die prior to extrusion. The concentric layers were unidirectionally oriented, as seen in the longitudinal section image in Fig. 2(b). The central axis of Al_2O_3–(m-ZrO_2) phase is the black contrast numbered 1 with the subsequent numbering for the outer cylindrical layers.

The thicker white contrast in Fig. 2(b) numbered 4 is the t-ZrO_2 outer layer of the cell, common to the adjacent unit cell. The inner t-ZrO_2 layers are marked accordingly. In the cross sectional image some cracks are evident at the interface of the lamina. In the processing steps we employed one low temperature burnout at 1000 °C for 2 h where paltry sintering occurs and the sample remains very weak. The residual stress development in the cooling stage in this step causes the cracking to begin, which on the subsequent high temperature sintering enhances. It is reported that the transverse and ''edge-effect'' cracking are due to the in plane tensile stress and can occur only if the laminate passes a critical thickness given by the equation, $t_c = 4K_{1C}^2/\pi\sigma_{R^2}$ [27]. Where, K_{1C} is the fracture toughness of the layer and σ_R is the residual stress. With the K_{1C}

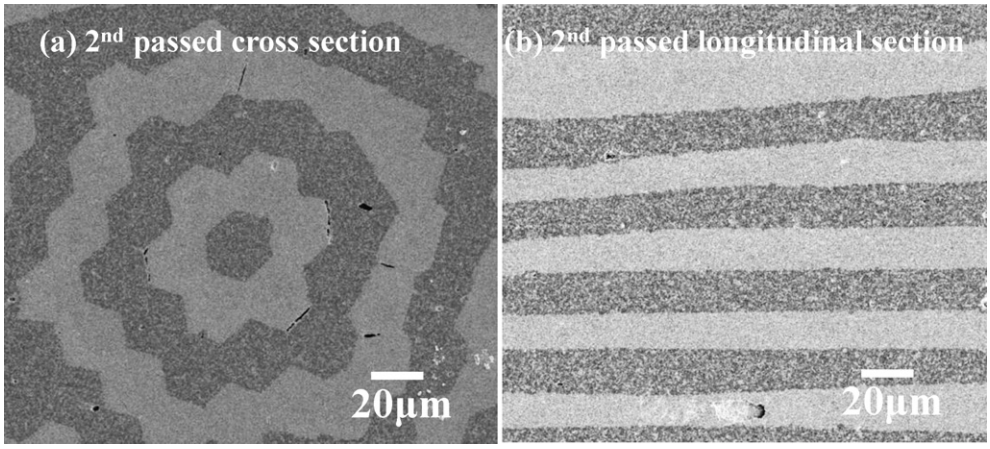

Fig. 2. SEM images of 2nd passed multilayer and fibrous Al_2O_3–(m-ZrO_2)/t-ZrO_2 composites sintered at 1500 °C.

value presumably being very low due to lack of densification at the low temperature sintering at 1000 °C, t_c for the layers are significantly reduced at this stage and is lower than the laminate thickness. However, the 3rd pass composites successfully eliminates this cracking with its fine layer thickness in the second burn out stage and subsequent high temperature sintering produces crack free and dense microstructure as shown in Fig. 3. However, due to the thinner dimension of the lamina in the 3rd pass sample the developed residual stress is also different and is expected to be lower, which in turn make the t_c higher for this finer microstructure.

Fig. 3(a) shows a cross sectional image of the 3rd passed sintered body. The unit cells of the concentric lamina groups were clearly observed in the figure bounded by the thicker white contrast representing t-ZrO_2. The unit cells were somewhat deformed from the hexagonal shape seen in the 2nd passed dense body. The unidirectional orientation of the lamina was unchanged and a very fine microstructure has been developed with parallel lamina, as shown in Fig. 3(c). Fig. 3(b) and (d) shows the enlarged cross section and longitudinal section images of the unit cell of the 3rd passed sintered composites. The layer thickness is almost uniform for t-ZrO_2 and Al_2O_3–(m-ZrO_2) layers in the cross and longitudinal section, but the interface was highly wavy in the cross section, whereas in the axial direction, it is finer and the lamina were almost equally spaced. The figures revealed that no processing defects like shrinkage cavities or interface cracks were found. The alternate multiple layers of t-ZrO_2 and Al_2O_3–(m-ZrO_2)

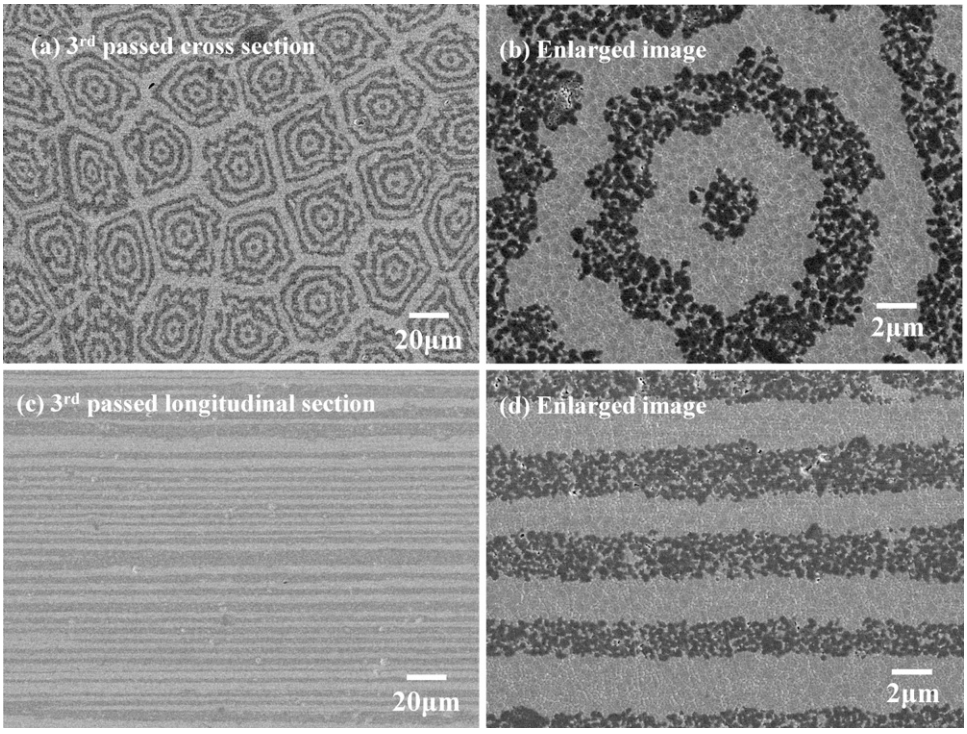

Fig. 3. SEM images of 3rd passed multilayer and fibrous Al_2O_3–(m-ZrO_2)/t-ZrO_2 composites sintered at 1500 °C.

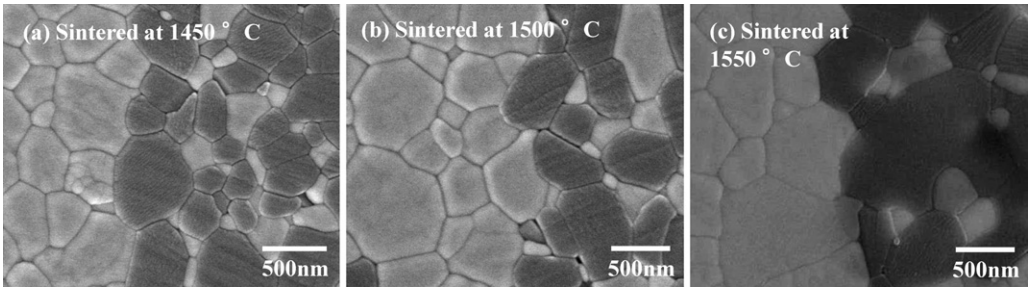

Fig. 4. Grain growth of the Al_2O_3 and ZrO_2 phase in the Al_2O_3–(m-ZrO_2)/t-ZrO_2 composites with sintering temperature.

were well-integrated and the interface of the two phases showed very good bonding without any failure. The interfaces in the enlarged images were shown to be intact without any cracks or de-bonding. Recent studies about laminated ceramics have shown improved strength and toughness with progressive layer refinement and disruption of planner connectivity of phases by a corrugated or wavy interface [28]. Because they provide more stress concentrators in the micro environment to trigger stress-assisted transformation for toughening functions. This corrugated interface was intentionally designed to improve the microstructural feature, and is attributed to the cylindrical shape of the individual monolithic green filaments that made the respective Al_2O_3–mZrO_2 and t-ZrO_2 layers in the feed arrangement prior to the 1st pass extrusion. This arrangement in the die before the 1st pass was the unit cell that ultimately got multiplied in the successive extrusion passes for the microstructure evolution. This was a unique aspect of this processing method.

Each ceramic layer in the frame region was in the range of 2–3 μm in thickness, which is thinner than the conventional tape cast laminated ceramic composites. The fine tuning of the microstructure can dramatically improve the high temperature performance of the composites. Usually the Al_2O_3 ceramics undergoes significant grain growth under prolonged high temperature exposure, which may deteriorate the mechanical properties of the ceramic body. In the present composites the microstructural dimension was less then 3 μm. This prohibits the grain growth of Al_2O_3 within this limit in the radial direction of the unit cell at prolonged elevated temperature exposure.

Fig. 4 shows the enlarged SEM image of the interface of the longitudinal section of the Al_2O_3–(m-ZrO_2)/t-ZrO_2 sintered body, subjected to different sintering temperatures from 1450 °C to 1550 °C. The grain growth was noticeable for both Al_2O_3 and ZrO_2 phases, but the growth of Al_2O_3 phase in the Al_2O_3–(m-ZrO_2) layer was retarded considerably by the ZrO_2 phase especially at 1450 °C temperature. Although all the grains underwent grain growth, almost all of them remained in the sub micrometer range. This was important for the ultimate mechanical performance of the composites. In all cases, the interface of the layers was intact, and neither interfacial de-bonding nor any other kind of processing defects were evident, as seen in the 3rd passed composites. However, a very small amount of intergranular pores were observed at lower sintering temperature which was removed at higher temperature.

Fig. 5 shows the XRD profiles of the Al_2O_3–(m-ZrO_2)/t-ZrO_2 composites in the (a) green composites, (b) after the 2nd burn out and (c) after sintering at 1500 °C. Fig. 5(c) shows that after sintering, the intensity of the m-ZrO_2 peak disappeared completely. This was because at temperature higher than 1200 °C, the m-ZrO_2 phase was transformed into t-ZrO_2 phase completely, and during densification this phase was entrapped in the Al_2O_3 phase and got stabilized. During the cooling time, the compact microstructure developed residual stress at lower temperatures where the Al_2O_3–(m-ZrO_2) layer fell under compressive stress due to the lower coefficient of thermal expansion (CTE) of this layer owing to the lower CTE of Al_2O_3 compared to that of the t-ZrO_2. As a result the t-ZrO_2 phase got stabilized under this compressive stress field in the presence of Al_2O_3 even at room temperature. However, the residual stress formation is also expected during the heating time when the laminates are first densified (differential densification). The phase stabilization behavior of m-ZrO_2 needs to be studied further which may reveal interesting outcome.

Table 1 shows the material properties of the sintered bodies obtained at different temperatures. All of the composites were highly dense and showed high bending strength values. The apparent fracture toughness was highest when sintered at 1500 °C and the value was 8.8 MPa $m^{1/2}$. The hardness value was highest when sintered at 1450 °C and decreased with increasing sintering temperatures. Higher grain growth at higher sintering temperatures contributed to the decreased bending strength and hardness. The fracture toughness showed a highest value when sintered at 1500 °C. From Fig. 4 it is evident that the grain growth is significantly prominent after

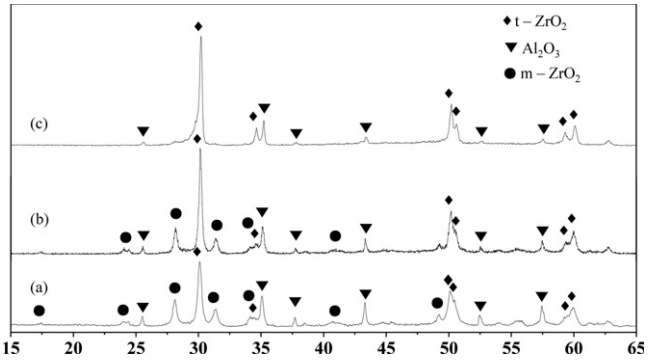

Fig. 5. XRD profiles of the Al_2O_3–(m-ZrO_2)/t-ZrO_2 multilayer composites at (a) green body, (b) after 2nd burn out and (c) after sintering at 1500 °C.

Table 1
Material properties of the Al_2O_3–(m-ZrO_2)/t-ZrO_2 composites.

Sintering temp. (°C)	Relative density (%)	Hardness (Hv)	Bending strength (MPa)	Fracture toughness (MPa $m^{1/2}$)
1450 °C	98.32	1413	923	7.1
1500 °C	98.78	1379	882	8.8
1550 °C	99.1	1365	867	8.0

sintering at 1550 °C than the other two temperatures. For a polycrystalline sintered t-ZrO_2 the grain boundary can modify the crack propagation behavior. With a small grain size the inter-granular crack travels rather intricate pathway. On the other hand with predominantly large Al_2O_3 grain the trans-granular pathway for crack is straighter and thus could extend further in case of indentation cracking. This was reflected in the fracture toughness of the composites sintered at three different temperatures. Fracture toughness essentially decreased from 1500 °C to 1550 °C as the grain growth for Al_2O_3 was significantly higher than that with the previous two.

The paths of crack propagation and its interaction with the microstructure are shown in Fig. 6 induced by the indenter. From the SEM images, it was clear that in both the cross section [Fig. 6(a) and (b)], and the longitudinal section [Fig. 6(c) and (d)], the direction of crack propagation was affected by the orientation of the microstructure. In the cross section, the crack path tried to bend along the interface of the two layers. The more tortuous crack of the crack propagation meant it had to go through a length while a portion of the crack propagation energy was dissipated by this process. This was translated in higher fracture toughness of the composites. In the longitudinal surface, the unidirectional alignment of the microstructure affected the crack propagation path and the crack propagation course was altered along the interface of the layers, as shown in Fig. 6(c). The crack path and interaction of the crack path with both the concentric and unidirectionally aligned layers of the microstructure were shown in two dimensional plans in the images. Due to the cylindrical geometry of each of the alternate layers, it is believed that the crack propagation path in 3D will interact more actively with the microstructure for both the concentric layered and unidirectional fibrous microstructure, as was evident in Fig. 6(a) and (c).

Fig. 7 shows the fracture surface of the concentric-multilayer Al_2O_3–(m-ZrO_2)/t-ZrO_2 composites sintered at 1500 °C. The fracture surface was taken from the broken sample filament after testing the bending strength. The surface shows the transverse surface normal to the cylindrical axis. Fig. 7(a) was taken from the 3rd passed sintered composites. The figure shows that the fracture surface was very rough and the alternate layers have significantly contributed to the roughness. In the enlarged SEM image of Fig. 7(b), it was clear that the layered microstructure had imparted a wavy surface area. This meant that the finely modified microstructure had interacted with the fracture propagation. Fig. 7(c) and (d) is taken from the Al_2O_3–(m-ZrO_2) and t-ZrO_2 layers, respectively and showed the enlarged view. In both layers the fracture mode was mainly inter-granular. In the t-ZrO_2 layer in Fig. 7(d), some t-ZrO_2 grains fractured in trans-granular mode, but the grain surface after fracture was very rough.

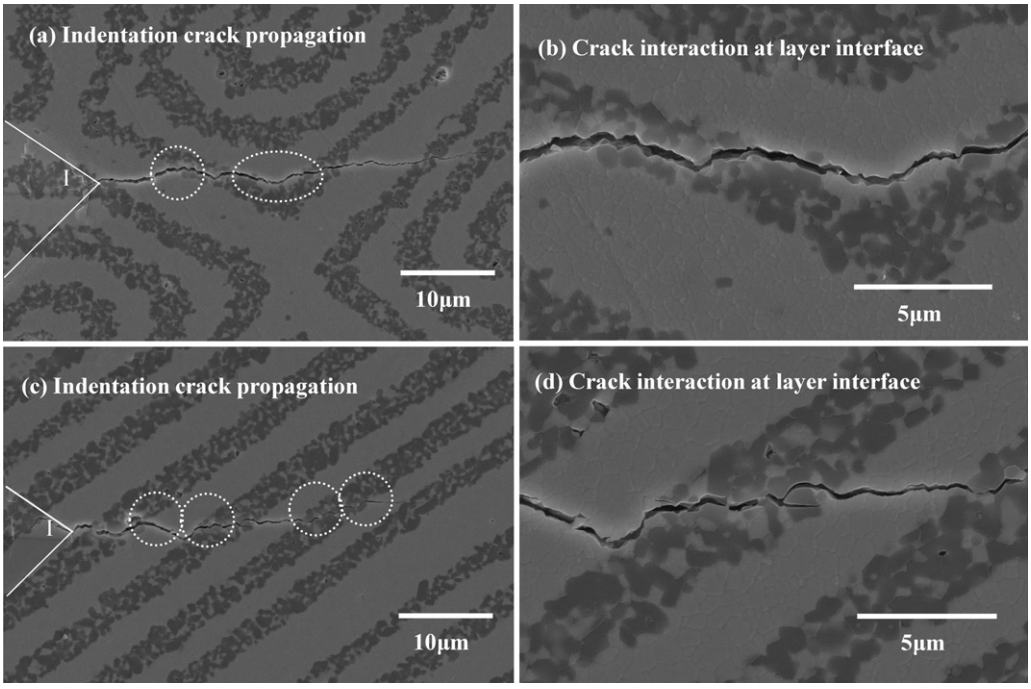

Fig. 6. Crack propagation behavior of Al_2O_3–(m-ZrO_2)/t-ZrO_2 multilayer composites sintered at 1500 °C.

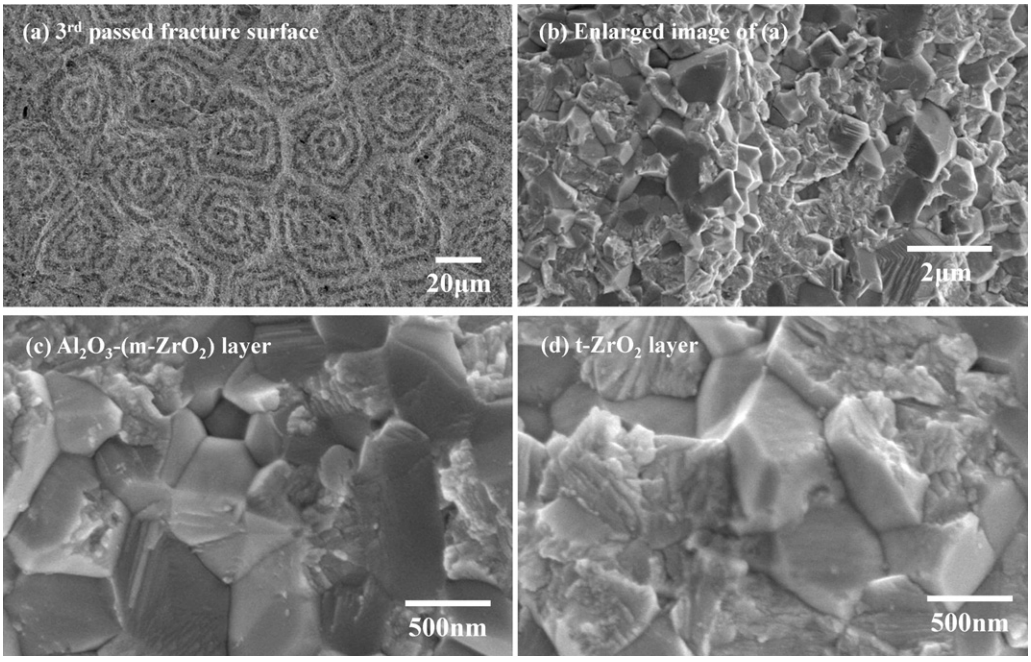

Fig. 7. Fracture surfaces of the concentric-multilayer Al_2O_3–(m-ZrO_2)/t-ZrO_2 composites sintered at 1500 °C.

4. Conclusions

A novel microstructure of Al_2O_3–(m-ZrO_2)/t-ZrO_2 composites with concentric multilayer was fabricated by a multi-extrusion process. The laminate thickness of the composites was as fine as 2–3 μm. In the composites, there were 7 alternate layers of t-ZrO_2 and Al_2O_3–(m-ZrO_2), which made a unit cell of unidirectionally aligned fibrous microstructure. The interfaces of the layers were corrugated in shape. The layers were integrated and produced homogeneous composites without any processing defects. The microstructure interacts with the crack propagation path and can alter the direction of propagation interpreting in higher fracture toughness. Due to the unique design and micro level dimension control, this type of microstructure can be modified using suitable functional materials to achieve various kinds of applications.

References

[1] B.T. Lee, A. Nishiyama, K. Hiraga, Micro-indentation fracture behavior of Al_2O_3–24 vol% ZrO_2 (Y_2O_3) composites studied by transmission electron microscopy, Mater. Trans. JIM 34 (88) (1993) 682–688.
[2] A.H.D. Aza, J. Chevalier, G. Fantozzi, M. Schehl, R. Torrecillas, Crack growth resistance of alumina, zirconia and zirconia toughened alumina ceramics for joint prostheses, Biomaterials 23 (3) (2002) 937–945.
[3] B.R. Lawn, Fracture of Brittle Solids, Cambridge University Press, 1993.
[4] P.F. Becher, Microstructural design of toughened ceramics, J. Am. Ceram. Soc. 74 (2) (1991) 255.
[5] F.F. Lange, Powder processing science and technology for increased reliability, J. Am. Ceram. Soc. 72 (1) (1989) 3–15.
[6] A.G. Evans, Perspective on the development of high-toughness ceramics, J. Am. Ceram. Soc. 73 (2) (1990) 187.
[7] W.J. Clegg, K. Kendall, N.M. Alford, T.W. Button, J.D. Birchall, A simple way to make tough ceramics, Nature 347 (1990) 455–457.
[8] D.B. Marshall, J.J. Ratto, F.F. Lange, Enhanced fracture toughness in layered microcomposites of Ce–ZrO_2 and Al_2O_3, J. Am. Ceram. Soc. 74 (12) (1991) 2979–2987.
[9] M. Oeschner, C. Hillman, F.F. Lange, Crack bifurcation in laminar ceramic composites, J. Am. Ceram. Soc. 79 (7) (1996) 1834.
[10] O.N. Grigoriev, A.V. Karoteev, E.N. Maiboroda, I.L. Berezhinsky, B.K. Serdega, D.Y. Ostrovoi, V.G. Piskunov, Structure, nonlinear stress-strain state and strength of ceramic multilayered composites, Compos. B-Eng. 37 (2006) 530–541.
[11] T. Chartier, D. Merle, J.L. Besson, Laminar ceramic composites, J. Eur. Ceram. Soc. 15 (1995) 101–107.
[12] A.J. Sánchez-Herencia, C. Pascual, J. He, F.F. Lange, ZrO_2/ZrO_2 layered composites for crack bifurcation, J. Am. Ceram. Soc. 82 (6) (1999) 1512–1518.
[13] R. Bermejo, C. Baudín, R. Moreno, L. Llanes, A.J. Sánchez-Herencia, Processing optimization and fracture behavior of layered ceramic composites with highly compressive layers, Compos. Sci. Technol. 67 (2007) 1930–1938.
[14] M.J. Melendo, F.G. Mora, A.D. Rodriguez, Effect of layer interfaces on the high-temperature mechanical properties of alumina/zirconia laminate composites, Acta Mater. 48 (2000) 4715.
[15] K.P. Plucknett, C.H. Cáceres, D.S. Willinson, Tape casting of fine alumina/zirconia powders for composite fabrication, J. Am. Ceram. Soc. 77 (8) (1994) 2137–2144.
[16] C.J. Russo, M.P. Harmer, H.M. Chan, G.A. Miller, Design of a laminated ceramic composite for improved strength and toughness, J. Am. Ceram. Soc. 75 (12) (1992) 3396–3400.
[17] J. Requena, R. Moreno, J.S. Moya, Alumina and alumina/zirconia multilayer composites obtained by slip casting, J. Am. Ceram. Soc. 72 (8) (1989) 1511–1513.
[18] J.S. Moya, A.J. Sánchez-Herencia, J. Requena, R. Morenon, Functionally gradient ceramics by sequential slip casting, Mater. Lett. 14 (1992) 333–335.
[19] A. Dakskobler, T. Kosmac, The preparation and properties of Al_2O_3–ZrO_2 composites with corrugated microstructures, J. Eur. Ceram. Soc. 24 (2004) 3351–3357.
[20] P. Sarkar, X. Haung, P.S. Nicholson, Structural ceramic microlaminates by electrophoretic deposition, J. Am. Ceram. Soc. 75 (10) (1992) 2907–2909.
[21] O. Prakash, P. Sarkar, P.S. Nicholson, Crack deflection in ceramic/ceramic laminates with strong interfaces, J. Am. Ceram. Soc. 78 (4) (1995) 1125–1127.

[22] R.J. Moon, M. Hoffman, K. Bowman, K. Trumble, Layer orientation effects on the R-curve behavior of multilayered alumina–zirconia composites, Compos. B-Eng. 37 (2006) 449.
[23] R. Bermejo, Y. Torres, L. Llanes, Processing optimisation and fracture behaviour of layered ceramic composites with highly compressive layers, Compos. Sci. Technol. 68 (1) (2007) 244.
[24] A.C. Seibi, M.F. Amateau, Finite element modeling and optimization for controlling the residual thermal stresses of laminated composite tubes, Compos. Struct. 41 (1998) 151–157.
[25] B.T. Lee, D.H. Jang, I.C. Kang, C.W. Lee, Relationship between microstructures and material properties of novel fibrous Al_2O_3–(m-ZrO_2)/t-ZrO_2 composites, J. Am. Ceram. Soc. 88 (10) (2005) 2874–2878.
[26] B.T. Lee, S.K. Sarkar, A.K. Gain, S.J. Yim, H.Y. Song, Core/shell volume effect on the microstructure and mechanical properties of fibrous Al_2O_3–(m-ZrO_2)/t-ZrO_2 composite, Mater. Sci. Eng. A 432 (1–2) (2006) 317–323.
[27] S. Ho, Z. Suo, Tunneling cracks in constrained layers, J. Appl. Mech. 60 (4) (1993) 890.
[28] M. Menon, I.W. Chen, Biomaterial composites via colloidal rolling techniques: III. Mechanical properties, J. Am. Ceram. Soc. 82 (12) (1999) 3430–3440.